



Contents lists available at ScienceDirect

## Materials Today: Proceedings

journal homepage: [www.elsevier.com/locate/matpr](http://www.elsevier.com/locate/matpr)

# Investigation on machining characteristics of T6-Al7075 during EDM with Cu tool in steady and rotary mode

B.C. Routara\*, Diptikanta Das, M.P. Satpathy, B.K. Nanda, A.K. Sahoo, Shubham S. Singh

School of Mechanical Engineering, KIIT Deemed to be University, Odisha, India

## ARTICLE INFO

### Article history:

Received 31 December 2019

Accepted 13 February 2020

Available online xxxx

### Keywords:

MRR

TWR

TOPSIS

$R_a$

$R_q$

## ABSTRACT

In this paper, aluminium alloy T6-Al7075 is machined using Electrical-discharge machining (EDM). For machining the material,  $L_9$  orthogonal array with three different levels of process parameters has been used. To study the machining performances three process variables, such as spark gap, pulse-off time and peak current have been selected. Metal removal rate (MRR), tool wear rate (TWR), roughness parameters  $R_a$  and  $R_q$  are considered as responses where tool is in steady and rotary mode. The multi-objective optimization for the responses have been analyzed using TOPSIS method. Furthermore, the investigation for surface texture has been carried out in both the machining condition. MRR increases in the case of tool in rotary mode than the steady mode.

© 2020 Elsevier Ltd. All rights reserved.

Selection and of the scientific committee of the 10th International Conference of Materials Processing and Characterization.

## 1. Introduction

Recently, most of the manufacturing industries are concerned over the quality of the product in terms of less dimensional deviation and good surface finish. For which, researchers are concentrated on different types of non-conventional machining operations, and Electrical discharge machining (EDM) is one them which is mostly used in industries like automobile and die-making sectors. In small intervals of time, a bunch of continuous discharges generated by RC generator inbetween two electrodes enhances the working zone temperature above the melting point of metal leading to removal of material from the work-piece. The particles eroded from work-piece are removed away by the dielectric with certain pressure. Generally, EDM is applied for machining of high strength material like T6-Al7075, which is also light in weight. Basically, T6-Al7075 is used in arms and aerospace industries for its high strength quality. Investigators are studied the influence of process variables on machining characteristics on EDM in stationary and rotary tool condition. Out of them few research papers are cited here to understand the past work for further research. Soni *et al.* has carried on an extensive study on machining of EN-8 with rotary tool EDM and suggested that metal removal rate enhances with increase in tool rotation [1]. Vincent

and Kumar studied the EDM behavior of En41b nitride steel using copper and brass rotary tubular electrode. The optimum set of process parameters has been identified by grey relational analysis [2]. Similarly, Teimouri and Baseri investigated the effect of magnetic field and rotation of tool in EDM process. The MRR and SR improves due to the magnetic field in and around the machining gap. The machining performance increases due to the rotational magnetic field in comparison of steady conditions [3]. Dwivedi and Choudhury measured the recast layer thickness of workpiece using tool in rotary and steady mode. It has been found that recast layer thickness reduces significantly in rotary tool phase as comparison to stationary tool [4]. Taguchi approach has been used by Aliakbari *et al.* in rotary EDM for optimizing machining parameters and suggested that electrical parameters are more significant than non-electrical parameter [5]. During the machining of AISI D3 steel by the rotation of tool, Dwivedi *et al.* found that a good surface finish is achieved as the rotation in the electrode enables uniform machining [6–7]. Singh *et al.* conducted an experiment using brass and copper tool to verify the effect of  $T_{off}/T_{on}$  on EDM during machining of AISI D3 and found that material removal rate rises with increase in pulse-off time and declines with increase in pulse-on time [8]. Pandey *et al.* [9] had investigated the cryogenic treated rotary copper-tool in EDM and concluded that tool wear became less whereas removal of material improved with better surface finish. Pushyanth *et al.* have investigated MRR during machining of AISI-D7 by EDM and concluded pulse-off-time ( $T_{off}$ )

\* Corresponding author.

E-mail address: [bcroutray@gmail.com](mailto:bcroutray@gmail.com) (B.C. Routara).

was the most significant factor for MRR than pulse-on-time ( $T_{on}$ ) [10]. The effect of magnetic field increases the MRR by 41.42% and surface finish improves by 2.17% as suggested by Anand *et al.* during machining in EDM [11].

Though lot many research papers published showing the influence of process variables on many responses, but very few papers show the importance of spark gap on responses like MRR and TWR on machining of T6-Al7075 alloy. In this work, an investigation has been done on process variables upon machining characteristics of T6-Al 7075 alloy using tool in steady and rotary condition, and multi characteristic optimization of process variables are studied.

## 2. Materials and method

Aluminium alloy T6-Al 7075 has been machined by EDM in the presence of kerosene as dielectric liquid in both machining condition, i.e. using Cu tool in steady and rotary mood. Workpiece of specimen size 100 mm  $\times$  45 mm  $\times$  10 mm is used for experimentation. The copper tool used for machining is with 99% of copper, and diameter of tool is about 19 mm.

Agiecharmiles FORM E-350 and S-350 Electro-discharge machines both made by GF machining solutions, Switzerland was used to machine the specimens in both steady and rotary mode respectively. For both the cases tool is negative polarity and workpiece is positive polarity. In rotary EDM tool speed is remain constant at 100 rpm. For proper positioning the workpiece the fixtures were used, as shown in Fig. 1 (a) and (b) for tool in steady and rotary modes, respectively.

Three factors with three levels were selected in this experimentation.  $L_9$  Orthogonal array is used as the design of experiment for experimentation. For conducting experiments, three machining parameters such as spark gap ( $d$ , mm), pulse off time ( $T_{off}$ ,  $\mu$ s) and peak current ( $I$ , Amp) have been selected. For both the machining environments, process variables and their levels remained same, as shown in Table 1. The arrangement of process parameters in coded and actual value along with experimental results are mentioned in Table 2 for steady mode of tool.

For calculating the material removal and tool wear rate, weight each of workpiece and tool are measured before and after the machining process. Figs. 2 and 3 show the camera photographs of work-pieces after machining in steady and rotary tool mode respectively.

After machining the work-pieces, the responses such as MRR, TWR and surface roughness parameters were measured. MRR and TWR were measured considering the weight loss before and after of each experiment. Surface roughness was measured in a surface roughness tester Mitutoyo SURFTTEST SV-2100, as shown in Fig. 4. The instrument uses a probe for surface roughness measurement which has a stylus consisting of a tiny diamond tip.

## 3. Results and discussion

### 3.1. Influence of steady tool and rotary tool machining

Measured experimental values for MRR, TWR,  $R_a$  and  $R_q$ ) are presented in the Tables 2 and 3, for stationary and rotary tool EDM, respectively. Experimental results reveal that MRR increased significantly for the tool in rotary mode with comparison to steady mode. It might be because of the tool rotation removed the eroded metal from working area and created the crater effectively, which is depicted in Fig. 5. Similarly, in rotary tool EDM, TWR increased as the tool rotation raised the spark intensity which led to increase in melting of work-piece due to the richness of spark, as shown in Fig. 6. The graphical representation of  $R_a$  is shown in Fig. 7. It is observed that the roughness value for the rotary tool is comparatively less than the steady tool, as rotation of tool distribute the spark uniformly in the machined surface. Similarly, the variation of roughness parameter  $R_q$  is shown in Fig. 8. It reveals that similar trend of nature for  $R_q$  in comparison to  $R_a$ .

### 3.2. Individual response optimization

#### 3.2.1. Tool in steady mode

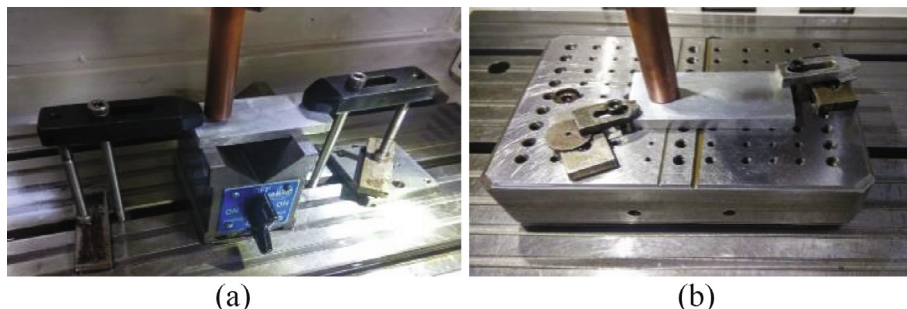
The responses are analysed on the basis of their characteristics like 'larger is better' or 'smaller is better'. For MRR, 'larger is better' criterion is chosen, and the main effect plots for S/N ratio for steady tool are shown in Fig. 9. With reference to Fig. 9 (a), the optimal set of parameters is the high level of spark gap, low level of pulse of time and mid-level of peak current which indicates the more MRR. To analyze TWR,  $R_a$  and  $R_q$ , the 'smaller is better' criteria has been chosen and the main effect plots for S/N ratio are shown in Fig. 9 (b)-(d). Fig. 9 (b) indicates that the optimal set of process variables for TWR is low level of spark gap, high level of pulse off time and high level of peak current. For roughness parameter  $R_a$ , the optimal combination of process parameter is low level of spark gap, low level of pulse off time and low level of peak current. Similar trend has also been observed for  $R_q$ .

#### 3.2.2. Tool in rotary mode

For machining in rotary tool, the responses are analyzed and the main effect plots for S/N ratios are shown in Fig. 10. Like steady

**Table 1**  
Levels of process variables.

Variables	Symbols	Levels		
		1	2	3
Spark gap (mm)	$d$	0.2	0.3	0.4
Pulse-off time ( $\mu$ s)	$T_{off}$	30	50	70
Peak current (Amp)	$I$	4	6	8

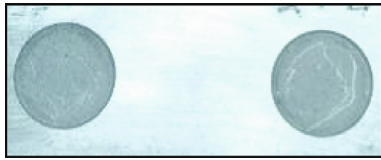


**Fig. 1.** Machining set-up (a) steady tool mode (b) rotary tool mode.

**Table 2**

Process parameter levels and experimental values for steady tool EDM.

Expt. no	Spark gap (mm)	Pulse-off time ( $\mu$ s)	Peak Current (Amp)	Spark gap (mm)	Pulse-off time ( $\mu$ s)	Peak Current (Amp)	MRR ( $\text{mm}^3/\text{min}$ )	TWR ( $\text{mm}^3/\text{min}$ )	$R_a$ ( $\mu\text{m}$ )	$R_q$ ( $\mu\text{m}$ )
1	1	1	1	0.2	30	4	0.03409	0.00239	3.8	4.7
2	1	2	2	0.2	50	6	0.03558	0.00101	4.5	5.6
3	1	3	3	0.2	70	8	0.02729	0.00064	4.2	5.3
4	2	1	2	0.3	30	6	0.04723	0.00248	4.0	5.0
5	2	2	3	0.3	50	8	0.04151	0.00147	4.5	5.6
6	2	3	1	0.3	70	4	0.02802	0.00184	4.1	5.1
7	3	1	3	0.4	30	8	0.04875	0.00254	4.3	5.5
8	3	2	1	0.4	50	4	0.04448	0.00133	4.5	5.7
9	3	3	2	0.4	70	6	0.03992	0.00132	4.1	5.3

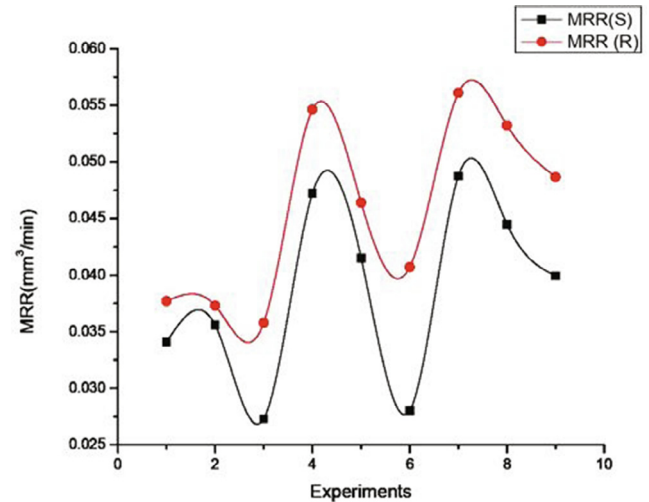
**Fig. 2.** Photos after machining of work-piece in steady mode of tool.**Fig. 3.** Photos after machining of work-piece in rotary mode of tool.**Fig. 4.** Surface roughness measurement by Mitutoyo SURFTEST SV-2100.

tool EDM process the optimal set of process variables for rotary tool EDM are selected with respect to the required characteristics of the responses. As per the Fig. 10 (a), the optimal combination for MRR is high level of spark gap, low level pulse off time and mid-level of peak current. For TWR, the optimal combination of parameter is low level of spark gap, mid-level of pulse off time and high level of peak current. Similarly, the optimal combination for  $R_a$  is low level of spark gap, high level of pulse off time and mid-level of peak current. In same way optimal combination of process parameters has been find out for  $R_q$ .

**Table 3**

Process parameter levels and experimental values for rotary tool EDM.

Expt. no	Spark gap (mm)	Pulse- off time ( $\mu$ s)	Peak Current (Amp)	Spark gap (mm)	Pulse-off time ( $\mu$ s)	Peak Current (Amp)	MRR ( $\text{mm}^3/\text{min}$ )	TWR ( $\text{mm}^3/\text{min}$ )	$R_a$ ( $\mu\text{m}$ )	$R_q$ ( $\mu\text{m}$ )
1	1	1	1	0.2	30	4	0.03769	0.00236	4.3	5.3
2	1	2	2	0.2	50	6	0.03729	0.00129	4.0	5.0
3	1	3	3	0.2	70	8	0.03579	0.00103	4.0	5.1
4	2	1	2	0.3	30	6	0.05462	0.0025	4.4	5.5
5	2	2	3	0.3	50	8	0.04641	0.00137	4.7	5.8
6	2	3	1	0.3	70	4	0.04070	0.00220	4.0	5.0
7	3	1	3	0.4	30	8	0.05610	0.00268	4.1	5.1
8	3	2	1	0.4	50	4	0.05322	0.00141	4.4	5.3
9	3	3	2	0.4	70	6	0.04865	0.00180	4.2	5.1

**Fig. 5.** MRR changes in different experimental runs using tool in steady and rotary mode.

ANOVA of the responses have been found out in both the case of steady and rotary tool EDM processes, and the summary is mentioned in Tables 4 and 5.  $R^2$ -value and optimal set of variables for both the machining conditions is cited also in Tables 4 and 5. It is found that pulse off time is significant for both MRR and TWR in steady tool EDM whereas peak current and pulse off time is significant for  $R_a$  and  $R_q$ .

### 3.3. Multiple response optimization

An optimal setting of process variables might be ideal for one quality attributes, yet it might be not reasonable for the other qualities. The multi-response improvement strategies are reasonable for these sorts of enhancement issues. For acquiring the multi-characteristics improvement of item quality, different methods have been created. One of them is Technique for Order Preference

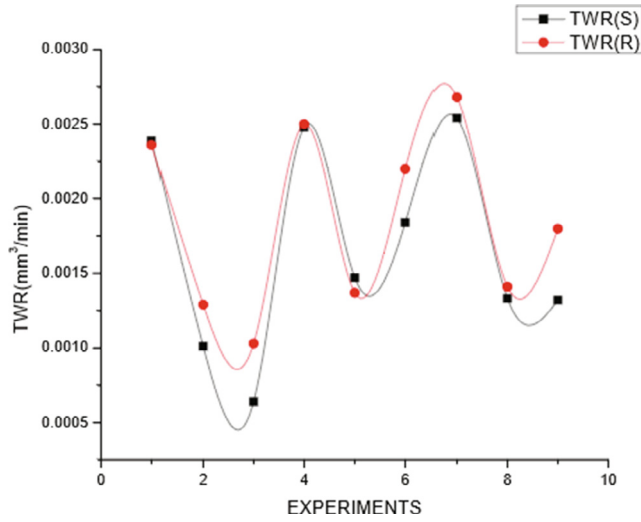


Fig. 6. TWR changes in different experimental runs using tool in steady and rotary mode.

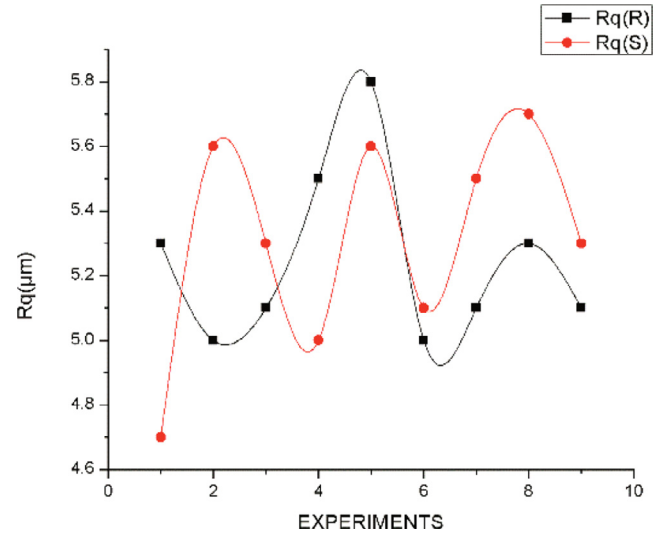


Fig. 8. Rq changes in different experimental run using tool in steady and rotary mode.

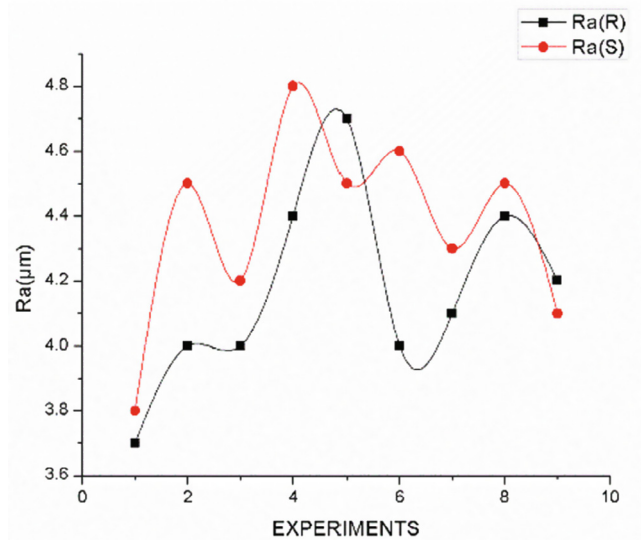


Fig. 7. Ra changes in different experimental run using tool in steady and rotary mode.

by Similarity to an Ideal Solution (TOPSIS) method. It is an analytical method for solving the multi objective problems to a single ideal solution by combining with the weightage of machining parameters depending upon the decision of the decision maker to get a feasible ideal solution. In this approach two artificial alternatives like positive and negative alternatives are hypothesized:

Positive ideal solution shows best level for all attributes taken into consideration.

Negative ideal solution shows the worst value.

TOPSIS finds the alternative which is the closest to the positive ideal solution and farthest from negative ideal solution.

Let  $x_{ij}$  value of option  $i$  with respect to criterion  $j$

$J$  be the set of benefit attributes whereas  $J'$  be the set of negative attributes

Step 1: Construct normalized decision matrix.

Normalize value as follows:

$$r_{ij} = x_{ij} / \sqrt{\sum x_{ij}^2} \text{ for } i = 1, \dots, m; j = 1, \dots, n \quad (1)$$

Step 2: Creation of the weighted normalized decision matrix. Weights are multiplied with each column of normalized decision matrix.

The next matrix is:

$$v_{ij} = w_j r_{ij} \quad (2)$$

Step 3: Finding of the positive ideal (best) and negative ideal (worst) solutions.

• Positive Ideal solution.

$$A^+ = \{v^1, \dots, v^{n+1}\} \quad (3)$$

where  $v_j^+ = \{\max(v_{ij}) \text{ if } j \in J; \min(v_{ij}) \text{ if } j \in J'\}$

• Negative ideal solution.

$$A^- = \{v^1, \dots, v^n\} \quad (4)$$

where  $v_j^- = \{\min(v_{ij}) \text{ if } j \in J; \max(v_{ij}) \text{ if } j \in J'\}$

Step 4: Compute the separation measures for each alternative.

• The separation from the positive ideal alternative is:

$$S_i^+ = \sqrt{\sum (v_j^+ - v_{ij})^2} \quad (5)$$

• the separation from the negative ideal alternative is:

$$S_i^- = \sqrt{\sum (v_j^- - v_{ij})^2} \quad i = 1, \dots, m \quad (6)$$

Step 5: Compute the relative closeness coefficient (CC) to the ideal solution  $C_i^+$

$$C_i^+ = \frac{S_i^-}{(S_i^+ + S_i^-)} \quad 0 < C_i^+ < 1 \quad (7)$$

Choose the option with  $C_i^+$  closest to 1.



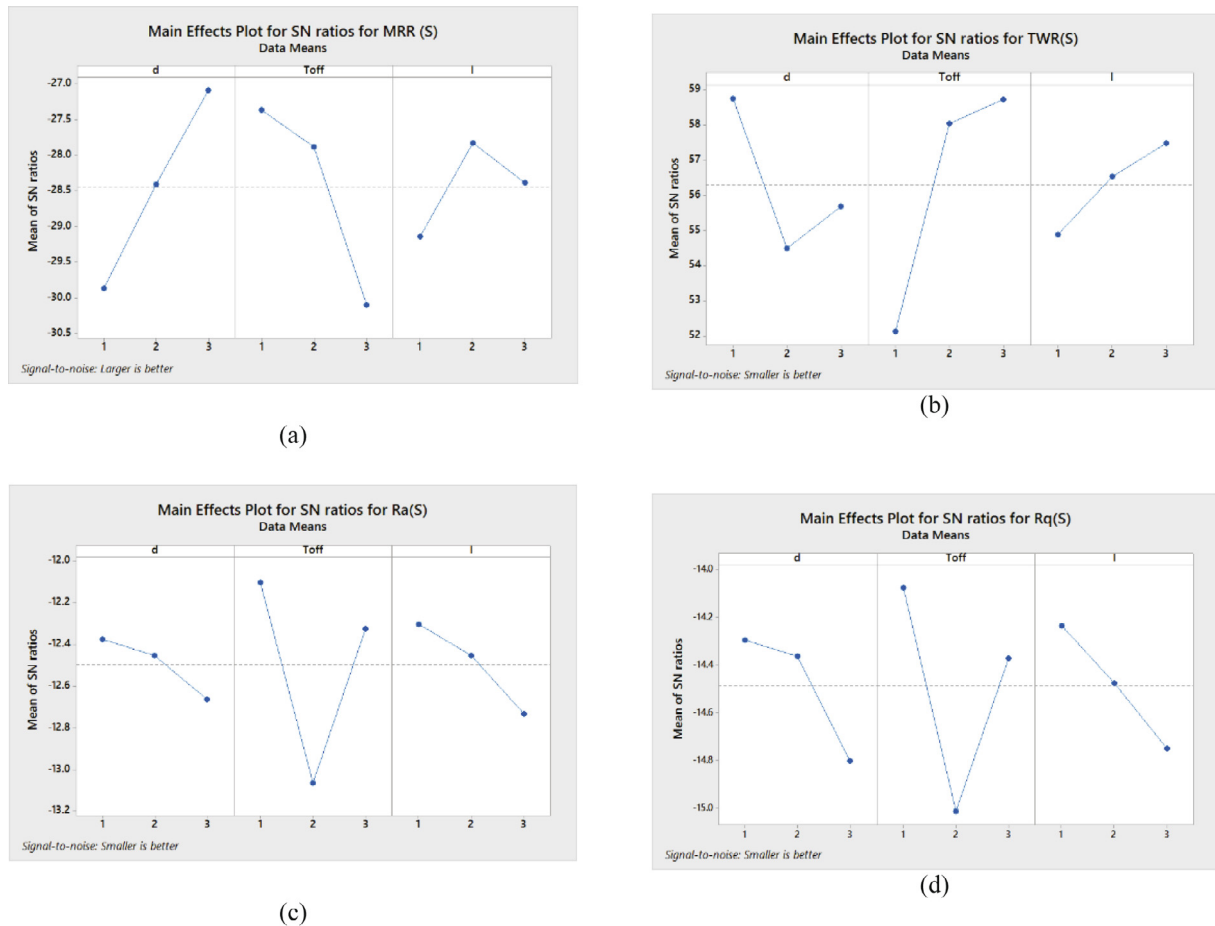


Fig. 9. Main effect plots for S/N ratio of (a) MRR (b) TWR (c) Ra (d) Rq for tool in steady mode.

### 3.3.1. Calculation of closeness coefficient in TOPSIS for stationary tool EDM

Step 1: The decision matrix of the responses is generated which is given in Table 2.

Step 2 Normalized decision matrix is developed using Equation (1) and shown in Table 6.

Step 3: Weighted normalized decision matrix formed using Equation (2) where  $w_j = 0.25$

Step 4: Positive ideal and Negative ideal solution for each element have been found using Eqs. (3)&(4).

For MRR positive ideal solution will be larger value, and for negative ideal solution it would be smaller value

For TWR,  $R_a$  &  $R_q$  positive ideal solution will be smaller value and for negative ideal solution it would be larger value.

Step 5: Using Eq. (5) & Eq. (6), the distances from positive ideal solution and negative ideal solution have been calculated as shown in Table 7.

Step: 6 Closeness coefficients are calculated using Eq. (7) and also shown in Table 7. The larger value of CC depicts that the specific set of process parameter is best among other set of experiments.

Hence from the above data we can see that the Run order 2 has the highest value of CC thus is the best optimal process parameter for the experiment.

### 3.3.2. ANOVA for close coefficient

The ANOVA for the closeness coefficient has been found at 95% of confidence level and it reveals that pulse off time is the most significant variable for multi objective characteristic and also the  $R^2$ -value is 96.97% which is very close to 1. The optimal set of process

variables for multi objective characteristic are low level of spark gap, high level of pulse off time and mid-level of peak current. The main effect plots for S/N ratio for stationary tool EDM is very much agreeing with ANOVA result Fig. 11. A confirmation test was performed on the above analysis and it has been found that closeness coefficient value has been improved. Hence, it may be concluded that multiple performance characteristics of stationary EDM can be improved by such approach.

### 3.3.3. Calculation of closeness coefficient for rotary tool EDM

Similar steps have been followed for finding out the closeness coefficient for rotary tool EDM process, and shown in Table 8. From the tabular data it can be revealed that the Run order 8 has the highest value of CC thus is the best optimal process parameter for the responses.

### 3.3.4. ANOVA for close coefficient

ANOVA for the closeness coefficient has been found at 95% of confidence level and it reveals that pulse off time is the most significant variable for multi objective characteristic and also the  $R^2$ -value is 92.47%, which is very close to 1. The optimal set of process variables for multi objective characteristic are high level of spark gap, mid-level of pulse off time and high level of peak current Fig. 12. The S/N ratio graph for stationary tool EDM is very much agree with ANOVA result. A confirmation test was performed on the above analysis and it has been found that closeness coefficient value has been improved. Hence it may be concluded that multiple performance characteristics of Stationary EDM can be improved by such approach.

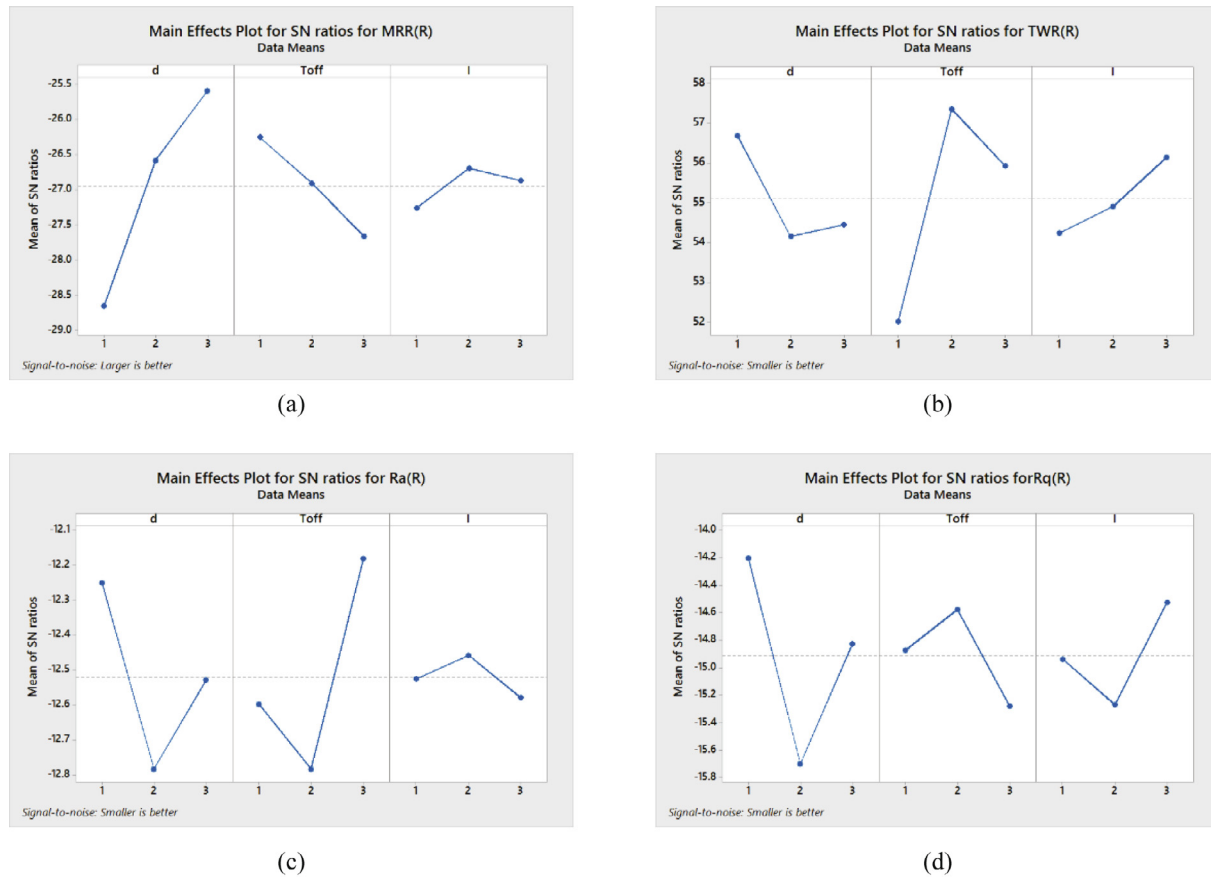


**Fig. 10.** Main effect plots for S/N ratio of (a) MRR (b) TWR (c) Ra (d) Rq for tool in rotary mode.

**Table 4**

Summary of ANOVA Table for responses in steady tool EDM.

Responses	Parameters	Significant (Yes/No)	R <sup>2</sup> -value	Optimal combination of parameters
MRR	Spark gap(mm)	Yes	98.5	d <sub>1</sub> Toff <sub>1</sub> I <sub>2</sub>
	Pulse-off time(μs)	Yes		
	Peak current(Amp)	No		
TWR	Spark gap(mm)	No	95.65	d <sub>1</sub> Toff <sub>3</sub> I <sub>3</sub>
	Pulse-off time(μs)	Yes		
	Peak current(Amp)	No		
R <sub>a</sub>	Spark gap(mm)	No	91.48	d <sub>1</sub> Toff <sub>1</sub> I <sub>1</sub>
	Pulse-off time(μs)	Yes		
	Peak current(Amp)	Yes		
R <sub>q</sub>	Spark gap(mm)	No	92.84	d <sub>1</sub> Toff <sub>1</sub> I <sub>1</sub>
	Pulse-off time(μs)	Yes		
	Peak current(Amp)	Yes		

**Table 5**

Summary of ANOVA Table for responses in rotary tool EDM.

Responses	Parameters	Significant (Yes/No)	R <sup>2</sup> -value	Optimal combination of parameters
MRR	Spark gap(mm)	Yes	95.41	d <sub>3</sub> Toff <sub>1</sub> I <sub>2</sub>
	Pulse-off time(μs)	No		
	Peak current(Amp)	No		
TWR	Spark gap(mm)	No	91.32	d <sub>1</sub> Toff <sub>2</sub> I <sub>3</sub>
	Pulse-off time(μs)	Yes		
	Peak current(Amp)	No		
R <sub>a</sub>	Spark gap(mm)	No	97.87	d <sub>1</sub> Toff <sub>3</sub> I <sub>2</sub>
	Pulse-off time(μs)	Yes		
	Peak current(Amp)	Yes		
R <sub>q</sub>	Spark gap(mm)	Yes	92.62	d <sub>1</sub> Toff <sub>2</sub> I <sub>3</sub>
	Pulse-off time(μs)	No		
	Peak current(Amp)	No		

**Table 6**  
Normalized decision matrix.

Experiment no.	MRR	TWR	R <sub>a</sub>	R <sub>q</sub>
1	0.291368	0.412069	0.289634	0.286236
2	0.304103	0.174138	0.342988	0.341048
3	0.233248	0.110345	0.320122	0.322777
4	0.403675	0.427586	0.365854	0.347138
5	0.354786	0.253448	0.342988	0.341048
6	0.239487	0.317241	0.35061	0.353228
7	0.416667	0.437931	0.327744	0.334957
8	0.380171	0.22931	0.342988	0.347138
9	0.341197	0.227586	0.3125	0.322777

**Table 7**  
Distance from positive and negative ideal solution.

Experiment no.	Distance measure from positive ideal solution (S <sub>i</sub> <sup>+</sup> )	Distance measure from negative ideal solution (S <sub>i</sub> <sup>-</sup> )	Closeness coefficient
1	0.081677	0.029941	0.268248
2	0.037576	0.068592	<b>0.646072</b>
3	0.047373	0.083041	0.636747
4	0.08304	0.042712	0.339655
5	0.043416	0.055609	0.361564
6	0.071766	0.030452	0.397915
7	0.083344	0.047056	0.360860
8	0.037115	0.064065	0.433178
9	0.036486	0.06107	0.625998

The bold indicates the highest closeness coefficient for steady and rotary tool EDM.

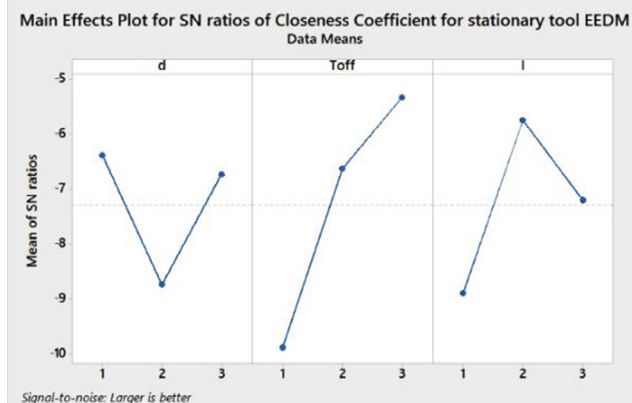


**Fig. 11.** Main effect plot for S/N ratio of closeness coefficient for steady tool EDM.

**Table 8**  
Closeness coefficient.

Experiment no.	Closeness coefficient
1	0.210869
2	0.653303
3	0.684274
4	0.338468
5	0.681314
6	0.331761
7	0.340503
8	<b>0.766793</b>
9	0.561234

The bold indicates the highest closeness coefficient for steady and rotary tool EDM.

### 3.4. SEM of machined surfaces

ZEISS-SUPRA 55 made by Carl Zeiss, German is used for scanning electron micrographs. For both the machining conditions,

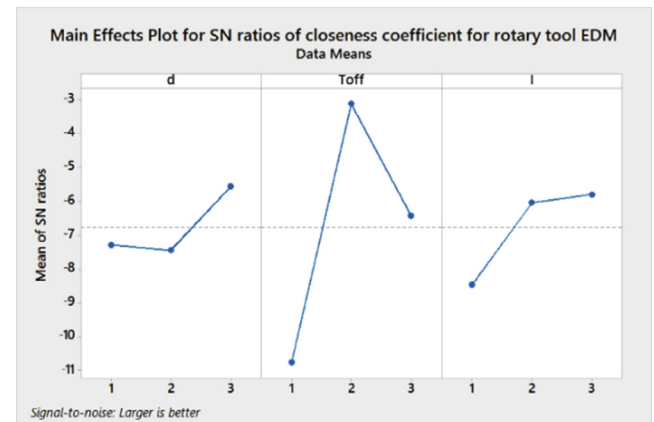


**Fig. 12.** Main effect plot for S/N ratio of closeness coefficient for rotary tool EDM.

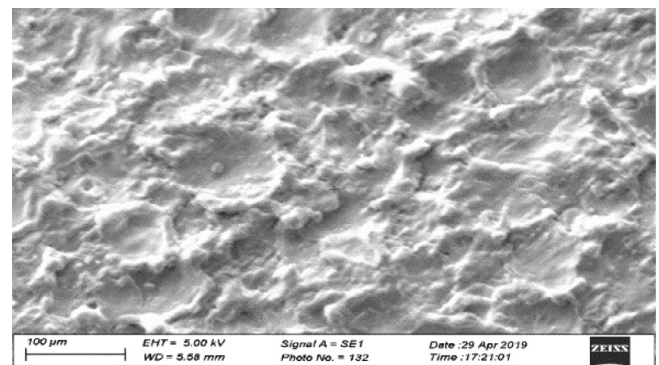


**Fig. 13.** Micrograph for steady tool EDM at optimal condition.

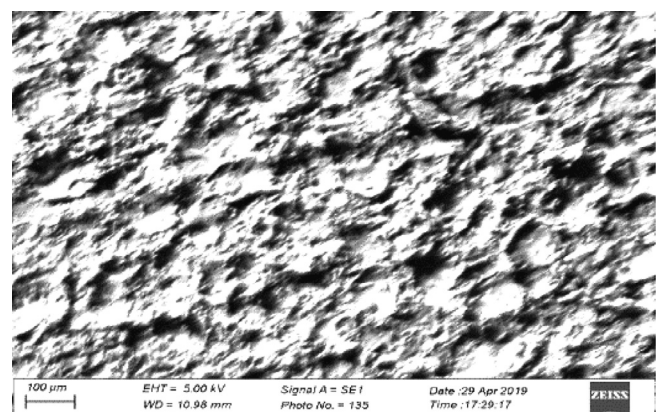


**Fig. 14.** Micrograph for rotary tool EDM at optimal condition.

micrographs taken for surfaces obtained by optimized value of process parameters. Surface texture for the tool in rotary mode provides better finish than tool in steady mode, which can be predicted from Figs. 13 and 14.

#### 4. Conclusions

Aluminium alloy T6-Al7075 is machined on EDM in both steady and rotary tool mode, and conclusions drawn are mentioned below.

- The material removal increases for the tool in rotary mode as compared to steady mode. Tool wear rate is comparatively less for the tool in rotary mode. However, the surface roughness parameters  $R_a$  and  $R_q$  are less in steady mood machining compared to the rotary mode.
- Significance of pulse-off time and spark gap is more for MRR in rotary and steady mode of tool. Pulse off time and peak current are significant parameters for  $R_a$  and  $R_q$  for both the machining condition.
- Multi objective optimization of process parameters are analysed using TOPSIS method. The optimal combination of process parameters for multi objective characteristic in steady tool EDM are low level of spark gap, high level of pulse off time and mid-level of peak current. Similarly, the optimal combination

of process parameters for multi objective characteristic in rotary tool EDM are high level of spark gap, mid-level of pulse off time and high level of peak current.

- SEM micrographs depict that surface texture is better in rotary tool mode than that of steady tool mode.

#### Declaration of Competing Interest

The authors declare that they have no known competing financial interests or personal relationships that could have appeared to influence the work reported in this paper.

#### References

- [1] M. Soni, R.J. Rana, A.B. Choudhury, *Int. J. Sci. Res. Sci. Techn.* 4 (8) (2018) 120–126.
- [2] N. Vincenta, A.B. Kumar, *Procedia Technol.* 25 (2016) 877–884.
- [3] R. Teimouri, H. Baseri, *J. Manuf. Process.* 14 (2012) 316–322.
- [4] A.P. Dwivedi, S.K. Choudhury, *Mater. Today Proceed.* 4 (2017) 10816–10822.
- [5] E. Aliakbari, H. Baseri, *Int. J. Adv. Manuf. Techn.* 62 (9–12) (2012) 1041–1053.
- [6] A.P. Dwivedi, S.K. Choudhury, *Trans. Engg. Techn.* (2016) 95–109.
- [7] A.P. Dwivedi, S.K. Choudhury, *Procedia Technol* 23 (2016) 280–287.
- [8] N.K. Singh, A. Poras, S. Das, *J. Int Engg. Techn.* 7 (3–12) (2018) 1154.
- [9] A. Pandey, R. Kumar, *Mat. Today Proceed.* 5 (2) (2018) 7635–7639.
- [10] V. Pushyanth, A. Bhaskar, *Mat. Today Proceed.* 5 (5) (2018) 12115–12123.
- [11] G. Anand, S. Satyanarayana, M. Hussain, *Mat. Today Proceed.* 4 (8) (2017) 7723–7730.